Geochimica et Cosmochimica Acta Vol. 51, pp. 847–855

0016-7037/87/$3.00 + .00

Dedolomitization in Na-Ca-Cl brines from 100° to 200°C at 300 bars

R. K. STOESSELL,[1] R. E. KLIMENTIDIS[2] and D. R. PREZBINDOWSKI[3]

[1]Department of Geology and Geophysics, University of New Orleans, New Orleans, LA 70148, U.S.A.
[2]Exxon Production Research Co., P.O. Box 2189, Houston, TX 77001, U.S.A.
[3]International Petrology Research, 3228 East 15th St., Tulsa, OK 74104, U.S.A.

(*Received July* 10, 1986; *accepted in revised form January* 5, 1987)

Abstract—Dedolomitization experiments were run at 300 bars for 7 to 8 weeks at 100°, 150° and 200°C in chloride brines containing 2 m (molal) Na, 0.5 m Ca, and (except for 1 experiment) 0.02 m Sr. The "ordered" dolomite dissolved and low-Mg calcite back precipitated as a replacement and/or rim cement of equant spar calcite crystals 10 to 50 μm in diameter. Between 100° and 200°C the mode of calcite formation changed from direct precipitation into void space produced by dissolving dolomite to pseudomorphic replacement of dolomite. The dedolomitization textures formed in these experiments are similar to those found in the rock record.

Solution compositions were monitored as a function of experimental time and imply that calcite-dolomite equilibrium was approached at 100°C and reached at 150° and 200°C. The final aqueous molality ratios of Ca:Mg were 14.2, 23.5, and 35.4, respectively, at 100°, 150°, and 200°C. The respective activity ratios, computed using Pitzer's model, were 14.3, 23.6, and 37.0, representing estimated equilibrium constants for the reaction:

$$Mg^{2+} + 2CaCO_3 = CaMg(CO_3)_2 + Ca^{2+}.$$

The estimated standard state enthalpy of reaction is 3.6 kcal between 150° and 200°C.

The empirical Sr distribution coefficient, $(Sr/Ca)_{solid}/(Sr/Ca)_{liquid}$, for the precipitated calcite was determined from micro-probe analyses of the calcite and solution data. The average coefficient values increased with increasing temperature, being 0.027 (±0.008 = s.d. of 19 measurements), 0.048 (±0.017 = s.d. of 19 measurements), and 0.063 (±0.013 = s.d. of 32 measurements), respectively, at 100°, 150°, and 200°C.

INTRODUCTION

THE TERM DEDOLOMITIZATION is used in this report to refer to the replacement of dolomite by calcite. Dolomite dissolution is followed by calcite precipitation. The precipitation can occur in pore space created by dissolution or directly adjacent to the dissolution boundary without the presence of significant intermediate void space.

Dedolomitization as a diagenetic process has been commonly associated with near-surface conditions (CHILINGAR, 1956; BRAUM and FRIEDMAN, 1969). Several authors have proposed dedolomitization in the presence of brines during burial diagenesis, *e.g.*, KATZ (1968), LAND and PREZBINDOWSKI (1981), BUDAI *et al.*, (1984); however, this was formerly thought to require high aqueous sulfate concentrations (RAO, 1969; KATZ, 1968). Most subsurface reservoir fluids have SO_4 concentrations ranging from 1 to a few hundred ppm (*e.g.*, see CARPENTER *et al.*, 1974; KHARAKA *et al.*, 1977). KASTNER (1982), BACK *et al.* (1983) and the results of this study indicate dedolomitization in Na-Ca-Cl brines requires significant Ca concentrations and not the presence of aqueous SO_4.

As discussed by LAND and PREZBINDOWSKI (1985) and STOESSELL and MOORE (1985), geochemists are not in agreement over the fluid compositions needed to transform dolomite to calcite during late diagenesis. In this study dedolomitization was produced in laboratory experiments involving Na-Ca-Cl brines between 100° and 200°C. The changes in fluid chemistry were monitored as a function of time and the texture and chemistry of the solids were determined using microanalytical techniques.

The study was designed with several goals: to measure the molality ratios of Ca:Mg at or near equilibrium between calcite and dolomite at diagenetic temperatures; to measure the Sr distribution coefficient in calcite; and to compare dedolomitization textures produced in the laboratory with those observed in thin sections of reservoir samples. We wanted to resolve some of the controversy obtained from different predictions of dolomite-calcite equilibrium based on the 25°C standard state data sets of ROBIE *et al.* (1979) and HELGESON *et al.* (1978); to provide data on Sr partitioning for use in modelling Sr mobility during diagenesis; and to set geochemical constraints on the occurrence of certain dedolomitization textures.

THERMODYNAMICS

The activity ratio of Ca^{2+}:Mg^{2+} at a particular pressure (P) and temperature (T) is constant for a fluid in equilibrium with both calcite and dolomite. This ratio is defined below by reaction (1):

$$2CaCO_2 + Mg^{2+}_{aq} = CaMg(CO_3)_2 + Ca^{2+}_{aq} \quad (1)$$

such that

$$K_1 = \frac{a_{Ca^{2+}}}{a_{Mg^{2+}}} = \frac{m_{Ca^{2+}}}{m_{Mg^{2+}}}\frac{\gamma_{Ca^{2+}}}{\gamma_{Mg^{2+}}} \quad (2)$$

where K_1 is the thermodynamic equilibrium constant for reaction (1). Calcite and dolomite are in their standard states and a_i, m_i, and γ_i represent the activity, molality, and activity coefficient, respectively, of the ith aqueous component. In this study γ_i will be computed as a stoichiometric activity

coefficient, hence m_i will always refer to the *total* molality of the ith species.

The change in the ln K_1 with temperature is given by the van't-Hoff's equation

$$\frac{\partial \ln K_1}{\partial(1/T)} = \frac{-\Delta H_r^0}{R} \quad (3)$$

where T is the temperature in °K, R is the ideal gas constant, and ΔH_r^0 is the standard state enthalpy of reaction. Equation (3) is used in this study to estimate ΔH_r^0 from experimental data at 150° and 200°C by neglecting any temperature dependence that ΔH_r^0 may have between the two temperatures.

The experimental molalities were converted to activities using Pitzer's specific ion-interaction model (PITZER, 1979), including the electrostatic unsymmetric mixing terms, to predict $\gamma_{Ca^{2+}}$:$\gamma_{Mg^{2+}}$. The model has been tested in complex brines at 25°C (*e.g.*, HARVIE and WEARE, 1980) and found to be consistent with measurements of activity coefficients in single-salt solutions at higher temperatures (*e.g.*, WOOD *et al.*, 1984). We neglected the trace concentrations of inorganic carbon while computing γ_i in the Na-Ca-Mg-Sr-Cl brines used in our experiments. We could not compute CO_3^{2-} activity and hence could not compute the activity products for either dolomite or calcite hydrolysis.

The single-salt parameters in Pitzer's model (with the exception of NaCl) were determined from a plot of these parameters *versus* temperature using the 25°C data from PITZER (1979) and the higher-temperature data of HOLMES *et al.* (1978) and HOLMES and MESMER (1981). The single-salt parameters for NaCl were computed from equations given by PITZER (1979). The temperature dependence of the common-ion binary-salt parameters are available for the $CaCl_2$-NaCl-H_2O system (HOLMES *et al.*, 1981) but not for $MgCl_2$-NaCl-H_2O systems. We used the 25°C common-ion binary-salt parameters listed by HARVIE *et al.* (1984) and assumed parameters not reported for Sr were equivalent to those of Ca. This procedure was assumed to produce less error than mixing 25°C and higher temperature binary-salt parameters.

Thermodynamic equilibrium lines, relating the $a_{Ca^{2+}}/a_{Mg^{2+}}$ in Eqn. (2) to temperature are shown on several figures. These equilibrium lines are referenced to the 25°C standard state data for minerals of either HELGESON *et al.* (1978) or ROBIE *et al.* (1979). Molar volumes and coefficients of the standard state heat capacity function needed to compute apparent standard state free energies of formation of minerals at higher temperatures were taken from HELGESON *et al.* (1978). The apparent standard state chemical potentials of Ca^{2+} and Mg^{2+} were computed using the 25°C aqueous standard state data for Ca^{2+} and Mg^{2+} in the Berkeley data bank (HELGESON, pers. commun., 1/83 SUPCRT update) and the Helgeson equations of state for standard state molal heat capacities and volumes of aqueous species (HELGESON *et al.*, 1981).

Sr PARTITIONING BETWEEN CALCITE AND A FLUID

The Sr distribution coefficient, D_{Sr}, is defined by Eqn. (4) for calcite and was measured in this study. This type of empirical coefficient is often used by geologists to predict elemental partioning in chemical processes.

$$D_{Sr} = \frac{(Sr/Ca)_{calcite}}{(Sr/Ca)_{aq.}} \quad (4)$$

where the ratios of Sr/Ca can represent concentration ratios or weight ratios.

Another commonly used coefficient is the distribution factor, b_{Sr}, defined by Eqn. (5):

$$b_{Sr} = \frac{(\text{wt.\% Sr})_{calcite}}{(\text{wt.\% Sr})_{aq.}}. \quad (5)$$

If D_{Sr} and b_{Sr} are measured at equilibrium then they are related to the equilibrium constant of the following exchange reaction:

$$Ca^{2+}_{aq.} + SrCO_{3\ calcite} = Sr^{2+}_{aq.} + CaCO_{3\ calcite} \quad (6)$$

where

$$K_6 = \left(\frac{m_{Sr}}{m_{Ca}}\right)_{aq.} \left(\frac{X_{CaCO_3}}{X_{SrCO_3}}\right)_{calcite} \left(\frac{\gamma_{Sr^{2+}}}{\gamma_{Ca^{2+}}}\right)_{aq.} \left(\frac{\lambda_{CaCO_3}}{\lambda_{SrCO_3}}\right)_{calcite}. \quad (7)$$

K_6 is the thermodynamic equilibrium constant for reaction (6) and X_i and λ_i are the mole fraction and activity coefficient, respectively, of the ith carbonate mineral in calcite. Equation (7) can be rewritten in terms of D_{Sr} and b_{Sr} because X_{SrCO_3}/X_{CaCO_3} in calcite is equal to the molar ratio of Sr:Ca in calcite.

$$K_6 \left(\frac{\lambda_{SrCO_3}}{\lambda_{CaCO_3}}\right)_{calcite} \left(\frac{\gamma_{Ca^{2+}}}{\gamma_{Sr^{2+}}}\right)_{aq.} = D_{Sr}^{-1}$$

$$= b_{Sr}^{-1} \frac{(\text{wt.\% Ca})_{calcite}}{(\text{wt.\% Ca})_{aq.}}. \quad (8)$$

Equation (8) illustrates the dependence of D_{Sr} and b_{Sr} on the solution and solid composition through the activity coefficient terms, and in the case of b_{Sr}, on the concentrations of Ca in both phases. Clearly, D_{Sr} should only be used to predict elemental partitioning in situations under conditions similar to those in which it was measured. The use of b_{Sr} should be discouraged because of the neglect of the aqueous Ca content in its computation.

REACTANTS AND REACTANT CONDITIONS

The experimental pressure and temperature (*PT*) conditions, amount of solid reactants and brine compositions are listed in Table 1 along with sample times and measured solution chemistries. Experiments (1) and (2) were run at 100°; Exp. (3), at 150°; and Exp. (4), at 200°C. The experiments were run for total times of about 1200 hours or 50 days. The 300 bar pressure was initially picked to correspond to an average hydrostatic gradient of 25°C/km at 100°C, assuming a surface temperature of 25°C. With the exception of Exp. (1), 15 grams of dolomite were reacted with 400 grams of brine. In Exp. (1) an additional 15 grams of calcite was included as a reactant.

Iceland spar calcite and two different dolomites were used in the experiments. The first dolomite, used in Exp. (1), was of unknown origin. The second dolomite was from Thornwood, New York, and was obtained from Ward's Natural Science Establishment. The reactant material was crushed and sieved to produce a size fraction between 1 and 2 mm and then washed in distilled water to remove fine-size particles. Both dolomites were ordered as shown by the relevant superlattice reflections in the X-ray diffraction patterns (GOLDSMITH and GRAF, 1958). Chemical compositions of the reactant material are listed in Table 2. These analyses are based on cation concentrations measured by atomic absorption (AA) spectroscopy on the acid-soluble fraction and the assumption that CO_3^{2-} was the only anion. Samples of the two dolomites

Table 1. Fluid compositions during dedolomitization experiments.*

Time hrs	Ca	Mg	Na	Sr	Cl	HCO_3
			molalities			
			Exp. 1: 100°C and 300 bars			
0	0.501	trace	2.042	n.m.	3.069	0.0001
102	0.530	0.0067	2.192	n.m.	3.239	trace
356	0.506	0.0166	2.094	n.m.	3.180	0.0002
576	0.507	0.0227	2.217	n.m.	3.167	0.0002
1291	0.487	0.0342	2.169	n.m.	3.191	0.0001
			Exp. 2: 100°C and 300 bars			
0	0.489	trace	1.944	0.022	2.934	trace
467	0.461	0.0164	1.969	0.021	2.933	0.0005
1042	0.440	0.0286	1.921	0.022	2.927	0.0005
			Exp. 3: 150°C and 300 bars			
0	0.500	trace	1.939	0.021	3.009	0.00004
265	0.526	0.0164	1.872	0.020	2.958	0.00006
598	0.522	0.0206	1.876	0.020	3.030	0.00009
935	0.493	0.0215	1.867	0.020	3.036	0.00006
1200	0.502	0.0214	1.888	0.020	3.054	0.00006
			Exp. 4: 200°C and 300 bars			
0	0.448	trace	1.995	0.018	2.924	0.00004
253	0.436	0.0107	2.002	0.018	2.917	0.00007
592	0.426	0.0113	1.935	0.018	2.891	0.00016
898	0.432	0.0117	1.986	0.018	2.901	0.00006
1260	0.435	0.0123	2.013	0.018	2.956	0.00004

n.m. not measured

* Exp. 1: 15 g calcite and 15 g dolomite with 400 g of 2 molal NaCl and 0.5 molal $CaCl_2$ under CH_4 gas.
Exps. 2, 3, and 4: 15 g dolomite reacted with 400 g of 2 molal NaCl, 0.5 molal $CaCl_2$, and 0.02 molal $SrCl_2$ under Ar gas.

used in this study are available on request from the senior author.

The brines were made up gravimetrically using reagent-grade chemicals and subsequently analyzed by AA to verify their contents. These data are listed in Table 1 and show minor discrepancies from their gravimetric values. When greater than the analytical accuracy, these differences are attributed to variations in the amount of water bound on the hydrated $CaCl_2$ and $SrCl_2$ salts used to make-up the brines.

EXPERIMENTAL PROCEDURE AND ANALYTICAL TECHNIQUES

The four experiments, (1)–(4), were run in a stainless steel LECO TEM-Pres vessel containing a 500 cm^3 titanium-lined cylindrical reaction chamber. The chamber's dimensions are approximately 6.25 cm by 16 cm. The 300 bars of pressure was supplied through a gas phase in the head space of the chamber. Methane (Matheson grade ultra-high purity—99.97 mole% pure) was used in Exp. (1), and argon (99.99 mole% pure, supplied by Monarc Welding Supplies in New Orleans) was used in the remaining experiments The gas pressure was maintained by a Haskel AG 125C single-stage compressor and was read by a Heise CM 32508 gauge with a dead weight accuracy of 1 bar.

Table 2. Chemical analyses of acid-soluble carbonate reactants in weight percent.

	Calcite*	Dolomite**	Dolomite***
CaO	55.47	30.58	30.58
MgO	0.25	21.50	21.14
SrO	0.0187	0.0046	0.0037
CO_2	43.81	47.47	47.08
Totals	99.55	99.55	98.80
molar Mg/Ca	0.006	0.98	0.96

CO_2 was calculated assuming the cations were balanced with carbonate.
* calcite used in Exp. 1, completely acid soluble.
** dolomite used in Exp. 1, completely acid soluble.
*** dolomite used in Exps. 2-4, containing an average 0.75 wt. % acid insoluble material.

An electric wire furnace, surrounding the reaction chamber and covered by an insulation jacket, was used to heat the chamber to the experimental temperatures. The thermostat control utilized thermocouples along the outside of the chamber. The temperature could be monitored within the reaction chamber using a thermocouple port opening into a closed tube extending into the chamber. The measured accuracy of the reaction chamber temperature is within 1 degree Celsius.

The vessel was rocked on a 90° cycle per second during Exp. (1) and at half that speed for the remaining experiments. The change in rocking speed did not significantly affect the reaction kinetics of dedolomitization between Exps. (1) and (2) which were run at the same temperature.

During an experiment, the aqueous solution in the chamber was sampled at different time intervals. Sampling was performed using a stainless steel sample loop (approximately 12 cm^3 volume) connected through a stainless steel valve to a titanium tube extending through the top of the vessel to within several cm of the chamber bottom. Gravity segregation prevented the reacting grains from being removed with the fluid during sampling. The pressure in the sample loop was maintained within 5 bar of the reaction pressure during the 10 minute sampling procedure. However, the temperature of the sample loop was not controlled. The procedure involved evacuating the sample loop, weighing it to within 0.01 grams, and filling it with distilled water. The loop was then carefully flushed with fluid from the chamber through a back-pressure regulator and reweighed. Approximately, 40 ml of fluid from the chamber was removed in flushing and filling the loop. The sample mass was determined using the mass difference between the evacuated and filled loop.

All solution dilutions were made on a mass basis. A 1:30 dilution with distilled water occurred when a sample was re-

moved from the sample loop by flushing with distilled water. Degassing of methane (Exp. 1) or argon (all other experiments) occured during the flushing. No correction was made for the mass of these inert gases in the solution due to their low solubilities in high salinity aqueous fluids (see MILLER and HILDEBRAND, 1968; WEISS, 1970; STOESSELL and BYRNE, 1982).

The diluted sample was filtered through a Whatman #42 filter paper at room temperature and pressure. Measured alkalinities were near detection levels. This suggests that if carbonate solids were present and dissolved prior to filtration, they had an insignificant effect on the major element chemistry. After further dilutions, cation concentrations were measured on a Perkin-Elmer 5000 AA spectrophotometer in which 1000 ppm excesses of K and Sr were added for Ca, Mg, and Na analyses (air-acetylene flame) and 1000 ppm excess K was added for Sr analyses (acetylene-nitrous oxide flame). Cl and HCO_3 in meq/liter were measured, respectively, with a Buchler 4-2500 chloridometer and by alkalinity titrations to a pH of 4.5 with an Orion 407A pH meter. Analyses in meq/liter were converted to ppm using densities measured with pycnometers. The assumed accuracies (estimated from precision measurements) of the reported data are within 3% for Ca, Mg, and Cl and 5% for Na and 5 to 10% for HCO_3.

The concentrations of the inert components, Na and Cl, were measured as a check for errors in the sampling and dilution procedure. The large error for HCO_3 analyses reflects the near trace concentrations of many of the measurements. Loss of CO_2 during degassing could have resulted in lowering alkalinity by carbonate precipitation. However, this is unlikely because of the simultaneous dilution of the sample during degassing. The 25°C pH values of the 1:30 diluted and unfiltered samples ranged between 5 and 6. Measurements of 25°C pH values on samples which had not been diluted and degassed could not be obtained with the experimental procedure.

Textures of the reacted and unreacted solids were examined by scanning electron microscopy and thin section petrography. Quantitative chemical analyses of the reacted solids were determined on polished thin sections using a Cameca Camebax electron microprobe. A suite of carbonate standards (calcite, dolomite, siderite, and rhodochrosite) and a strontium sulfate standard (celestite) were used as reference samples. The solids from the experiments were analyzed as an accelerating voltage of 20 Kv and a specimen current of 10 nano-amperes. A one to ten μm spot size and short counting times (Ca, 10 sec; Fe, Mn, and Mg, 30 sec; Sr, 60 sec) were used to minimize volatilization. The calculated lower limits of detection for Sr and Mg were 390 and 290 ppm, respectively, for the conditions used in the analyses.

EXPERIMENTAL RESULTS AND DISCUSSION

Calcite-dolomite equilibria

During the experiments, a rim of low-Mg calcite, 10 to 50 μm thick, formed around the dissolving dolomite grains which were 1 to 2 mm in diameter. The precipitate was identified by X-ray diffraction on bulk powder mounts of reacted grains from Exps. (2)–(4). Calcite was included as a reactant in Exp. (1), preventing a positive identification of the precipitate as calcite. However, the common crystal morphology as determined from scanning electron microscopy and the cation determination by microprobe analyses indicate a low-Mg calcite precipitated in all the experiments with an average Mg content of about 720 ppm. The reacted grains were examined by petrographic examination of thin sections of the reacted grains. The mineral textures produced by the coupled dissolution and precipitation process are described later.

Rates of changes in solution composition, with respect to reaction time, decreased with increasing time reflecting the gradual approach to equilibrium between calcite and dolomite. Molality ratios, computed from the data in Table 1, are plotted as a function of reaction time in Figs. 1A, 1B, and 1C, respectively, for the experiments at 100°, 150°, and 200°C. The ratios are plotted as m_{Mg}/m_{Ca} in linear space, rather then the conventional log (m_{Ca}/m_{Mg}) values, to allow all of the

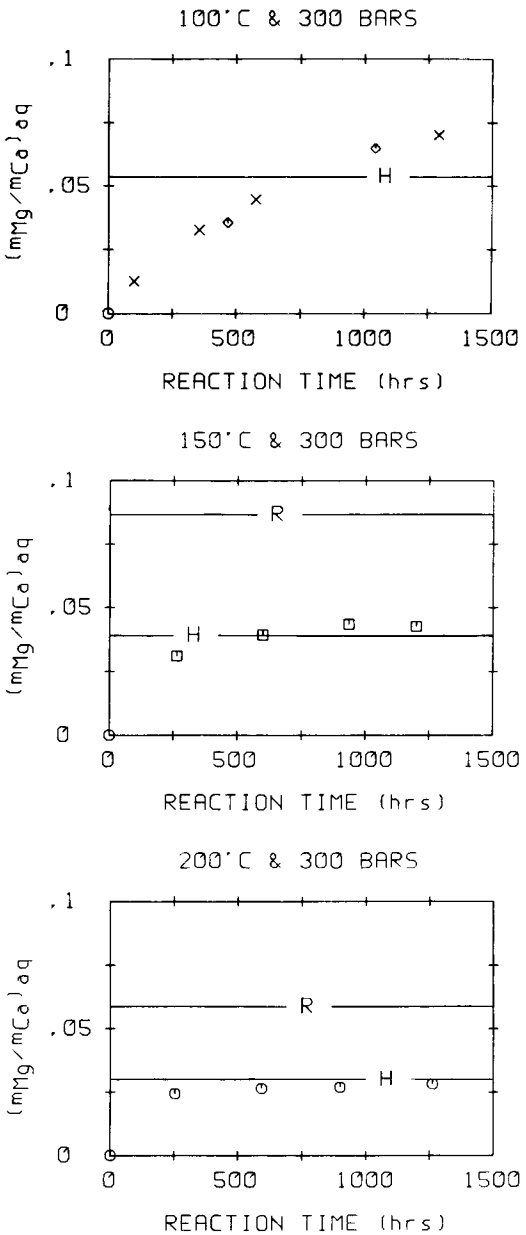

FIG. 1. m_{Mg}/m_{Ca} plotted *versus* reaction time in hours. Data from Exp. (1), ×, and Exp. (2), ◇, are shown on Fig. 1A; data from Exp. (3), □, are plotted on Fig. 1B; and data from Exp. (4), ○, are shown on Fig. 1C. The lines marked "H" and "R", respectively, represent equilibrium values between ordered dolomite and calcite referenced to the standard state data given by HELGESON *et al.* (1978) and ROBIE *et al.* (1979).

solution data to be represented on the same plot. The trends of the data imply equilibrium was approached at 100°C and reached at 150° and 200°C. The overlap in trends at 100°C with data from Exps. (1) and (2) indicate aqueous Sr had little or no effect on the reactions.

The predicted aqueous activity ratios of Mg^{2+}:Ca^{2+} for calcite-ordered dolomite equilibria, referenced to either the 25°C standard state data of ROBIE *et al.* (1979) or HELGESON *et al.* (1978), are also plotted on the figures. Pitzer's model predicts nearly identical activity coefficients for Ca and Mg in the brines used in this study. For this reason the molality ratios plotted on Figs. 1A, 1B, and 1C can be considered nearly equivalent to the corresponding activity ratios.

The Mg content of the brines in Exps. (1) and (2) may have continued to increase if the experiments had run for a longer time. The 100°C experiment should have been followed for a reaction time of 2000 hours (approximately 3 months). The mechanical wear in our system did not allow such long experiments. A linear inverse time extrapolation of the molality ratios at 100°C could be used to predict a molality ratio of Ca:Mg at infinite time. However, the use of such an extrapolation is a subject of controversy (see LAFON, 1978), arbitrarily assuming a hypothetical rate law.

Our 300 bar solution data representing the maximum reaction times at 100°, 150°, and 200°C are plotted as log ($a_{Ca^{2+}}/a_{Mg^{2+}}$) *versus* temperature on Fig. 2 together with several thermodynamic and empirical equilibrium curves for calcite-dolomite equilibria. The three log activity equilibrium curves are referenced to the 25°C data (calometric) of ROBIE *et al.* (1979) for calcite and dolomite and the data (retrieved from laboratory studies and computations on the effect of ordering) of HELGESON *et al.* (1978) for calcite and ordered dolomite and for calcite and disordered dolomite. The curves are computed for the experimental pressure of 300 bars, but they shift insignificantly if the pressure is allowed to vary with the temperature on an average hydrostatic gradient of 25°C per km. The log molality equilibrium line from LAND and PREZBINDOWSKI (1985) is a straight line connecting the molality ratios of Ca:Mg of the groundwater data (below 25°C) of LANGMUIR (1971) with a portion of the experimental data (between 350° and 400°C) of ROSENBERG and HOLLAND (1964) and ROSENBERG *et al.* (1967).

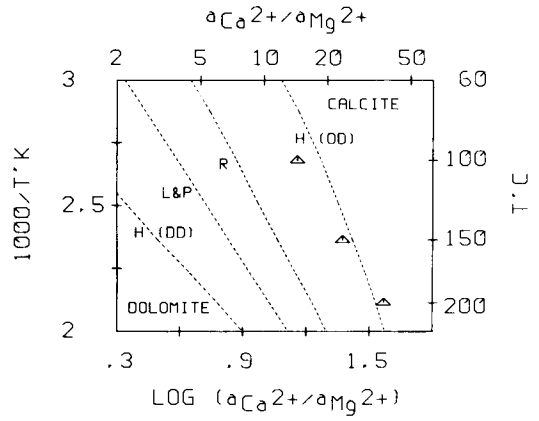

FIG. 2. Log ($a_{Ca^{2+}}/a_{Mg}$) plotted *versus* $1000/T$ where T is in °K. The three experimental data points, △, represent maximum reaction times at the three experimental temperatures. The dashed lines represent equilibrium between dolomite and calcite. The 300 bar lines labeled R, H(OD), and H(DD) are referenced, respectively, to the standard state data of ROBIE *et al.* (1979), and to the standard state of HELGESON *et al.* (1978) for ordered dolomite and disordered dolomite. The line labeled LP was taken from LAND and PREZBINDOWSKI (1985).

The experimental log ($a_{Ca^{2+}}/a_{Mg^{2+}}$) values plotted on Fig. 2 are 1.16, 1.37, and 1.57, respectively at 100°, 150°, and 200°C. Close agreement exists with the equilibrium curve for calcite and ordered dolomite using data taken from HELGESON *et al.* (1978). The corresponding 300 bar values are 1.27, 1.41, and 1.52, respectively, at 100°, 150°, and 200°C, respectively. These are unreversed experiments in which the activity ratios of Ca^{2+}:Mg^{2+} represent "maximum possible" equilibrium values. However, the absence of significant changes in solution composition with time near the end of the experiments at 150° and 200°C is a strong indication that equilibrium was reached. We emphasize that ordered dolomites may have a range of stabilities due to lattice defects (REEDER, 1981) and more experimental data are needed to check this possibility.

ΔH_r^0, computed from Eqn. (3) for reaction (1), is 3.6 kcal for the temperature range of 150° to 200°C. The average value decreases to 3.3 kcal if the experimental data from 100°C is included.

The only other published experimental study in this temperature range is by BAKER and KASTNER (1981). They report a value of −0.02 for the log (m_{Ca}/m_{Mg}) at the end of a two week experiment at 200°C in which calcite was converted to dolomite. The value plots off of Fig. 2 and is too low to be consistent with any of the equilibrium curves on Fig. 2.

Sr distribution coefficient in calcite

The data in Table 1 indicate the Sr/Ca ratio in the fluid remained nearly constant during Exps. (2), (3), and (4). The overall decreases in Sr and Ca in the fluid due to dolomite dissolution and calcite precipitation were minor because of the large reservoir of these components in the fluid. D_{Sr} was computed using the average molar fluid ratio in the samples taken during an experiment and microprobe analyses on the Sr content in the calcite rims on the dolomite grains. Multiple spot analyses were made on the calcite rims of several reacted grains in each experiment. Sr contents were below detection levels in the calcite precipitated in Exp. (1) reflecting the absence of significant aqueous Sr.

The average Sr content in ppm in the rim calcite was 1144 (±317 = s.d. for 19 measurements), 1629 (±589 = s.d. for 19 measurements), and 2269 (±474 = s.d. for 32 measurements), respectively, at 100°, 150°, and 200°C. The corresponding values of D_{Sr} are

0.027 (±0.008 = s.d. of 19 measurements), 0.048 (±0.017 = s.d. of 19 measurements), and 0.063 (±0.013 = s.d. of 32 measurements). The average D_{Sr} value more than doubles between 100° and 200°C; however, the standard deviation of the average value at each temperature ranges from 20% at 200° to 35% at 150°C. These large standard deviations imply Sr partitioning is not at equilibrium, but is controlled by reaction kinetics.

D_{Sr} values from this study are plotted on Fig. 3 together with D_{Sr} values from HOLLAND *et al.* (1964), KATZ *et al.* (1972), and LORENS (1981). D_{Sr} was reported by HOLLAND *et al.* to be 0.076 at 98°C for the direct precipitation of calcite from solution. The high value apparently is due to the inclusion of more Sr in a rapidly precipitating phase (LORENS, 1981). Average values reported by KATZ *et al.* at 40° and 98°C were 0.055 and 0.058, respectively, for calcite replacing aragonite. The Sr:Ca solution ratio varied during their runs, necessitating back-calculation of a value to best-fit the data. Our value at 100°C, 0.027, is 50% lower than that measured by Katz, presumably reflecting the slower replacement process involving dolomite. The effect of rates of calcite formation on D_{Sr} have been determined by LORENS (1981) at 25°C. He reports a value of 0.027 (±0.011) for recrystallized calcite.

JACOBSON and USDOWSKI (1976) report b_{Sr} values of 0.09 and 0.11 at 150 and 200°C, respectively, in calcite produced by dedolomitization. The authors did not report the Ca content of the calcite and aqueous solution, needed to compute D_{Sr}. The solution ratio of Sr:Ca is neglected in computing b_{Sr} (see Eqn. (5)). Our b_{Sr} values at 150° and 200°C are 1.09 and 1.68, respectively, apparently reflecting differences in solution ratios of Sr:Ca between the two studies.

DEDOLOMITIZATION TEXTURES

Dedolomitization textures produced during Exps. (2), (3), and (4) at 100°, 150°, and 200°C, respectively, are shown on Figs. 4 and 5. Textures produced during Exp. (1) are not shown because they were similar to those developed during Exp. (2). The increase in stability of dolomite relative to calcite with increasing temperature, resulted in a decrease of both dolomite dissolution and calcite precipitation.

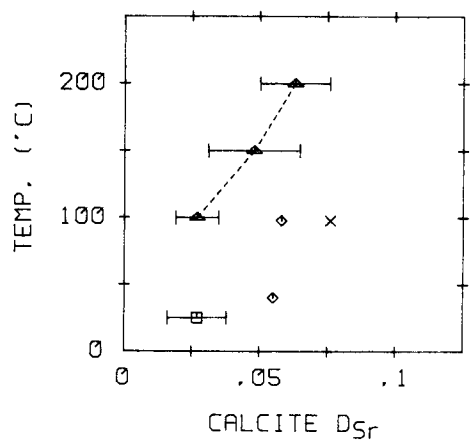

FIG. 3. D_{Sr} in calcite plotted *versus* temperature in °C. The data are from HOLLAND *et al.* (1964), ×; KATZ *et al.* (1972), ◇; LORENS (1981), □; and from this study, △. One standard deviation is indicated by the error bars on D_{Sr} reported from this study.

Exp. (2) at 100°C and 300 bars, Figs. 4A–4D

Calcite rims on the dolomite consist of euhedral crystals approximately 50 μm in diameter. The calcite is in optical continuity with the core-dolomite crystals. The nucleation sites for the euhedral calcite crystals appear to be the irregular pinnacles on the dolomite surface, formed during the early stages of dolomite dissolution (Figs. 4C and 4D). The remanents of these pinnacles commonly form irregular dolomite inclusions in the cores of the calcite crystals (Fig. 4A). The presence of the delicate-looking dissolution features on the dolomite implies dissolution rates were controlled by surface reactions (BERNER, 1981). The primary growth direction for the calcite was outward rather than as a pseudomorphic replacement of the dolomite (Figs. 4A and 4B).

Exp. (3) at 150°C and 300 bars, Figs. 5A and 5B

The euhedral calcite crystals are similar in size and morphology to those formed in Exp. (2). They completely cover the dolomite dissolution surface (Fig. 5B) and are in optical continuity with the core-dolomite crystals. The multiple-calcite crystal replacement of the coarsely crystalline dolomite and the remanent dolomite inclusions in the calcite crystals are similar to those resulting from dedolomitization in Exp. (2). However, there is a tendency for the calcite-dolomite interface to be more rounded, suggesting an increasing importance of pseudomorphic replacement of the dolomite (Fig. 5A).

Exp. (4) at 200°C and 300 bars, Figs. 5C and 5D

Anhedral calcite crystals have pseudomorphically replaced the outer 10 to 20 μm of the dolomite crystals as shown in the backscatter electron imagery (Fig. 5C). This replacement was initiated from the exterior of dolomite crystals, but internal dedolomitization associated with crystal defects has become evident. The rounded calcite-dolomite boundaries and the distribution of calcite in association with crystal imperfections such as fluid inclusion cavities support a pseudomorphic replacement origin for the calcite. The irregular and rounded dolomite inclusions floating in the calcite represent islands of unreplaced dolomite.

The dissolution textures at the interface of the calcite and dolomite lack the pinnacles and other features observed at the lower temperatures. This texture is believed to be the result of pseudomorphic replacement of partially dissolved dolomite by calcite.

We believe that dissolution may be controlled by diffusion within the "thin film" separating the calcite

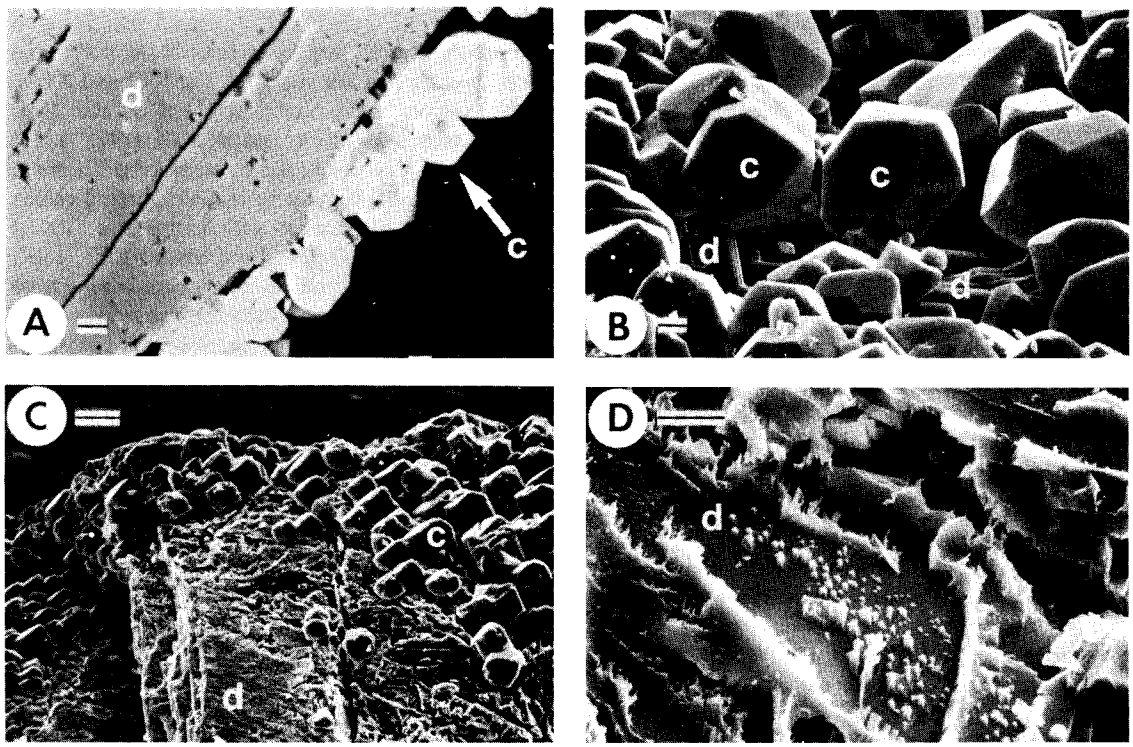

FIG. 4. Backscatter (4A) and secondary electron photomicrographs (4B, 4C, 4D) of dedolomitization mineral textures formed during Exp. (2) at 100°C. Scale bar equals 10 μm except in 4C where it equals 50 μm. The symbols d and c represent dolomite and calcite, respectively.

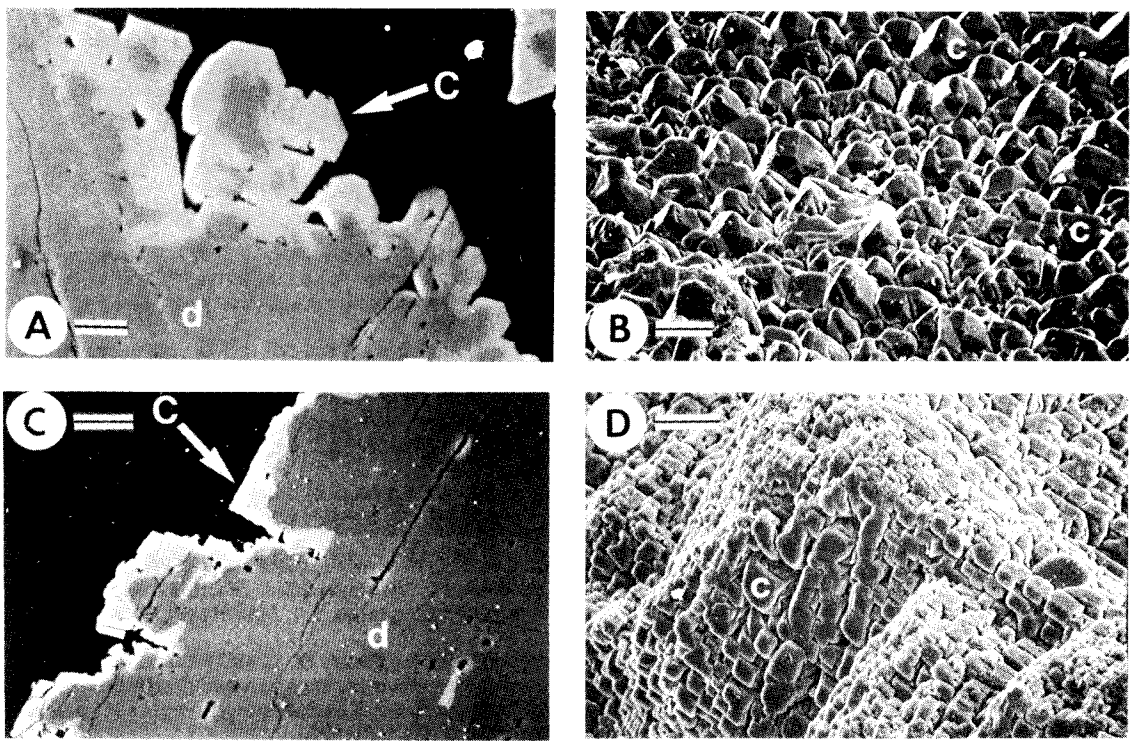

FIG. 5. Backscatter (5A) and secondary electron photomicrographs (5B) of dedolomitization mineral textures formed during Exp. (3) at 150°C, and backscatter (5C) and secondary electron photomicrographs (5D) of dedolomitization mineral textures formed during Exp. (4) at 200°C. The scale bar equals 25 μm on 5A and 5C and 50 μm on 5B and 5D. Calcite and dolomite are represented by c and d, respectively.

and dolomite. Components, released during dissolution and not reprecipitated, must diffuse through this thin film to reach the bulk fluid. No diffusional gradients exist in the bulk fluid because of the rocking motion of the reaction vessel. The change in dissolution control with increasing temperature implies a greater overall increase in the rate of surface reactions relative to the increase in the diffusion coefficients. In addition, the long path length of diffusion in the thin film increases the probability that transport removal would be the rate-controlling process.

Comparison of dedolomitization textures produced in the laboratory and observed in reservoir samples

Textural evidence for dedolomitization in reservoir samples include (1) irregular dolomite inclusions in calcite, (2) pseudomorphic calcite crystals after individual dolomite rhombs, (3) ghost of former rhombic dolomite crystals evidenced by mineral inclusions or crystal boundaries within calcite crystals, (4) a medium to coarse crystalline, dense dolomitic limestone with a cavernous and blistered appearance (RAO, 1969). The first three textural criteria are considered the most reliable indicators of past dedolomitization events. Each of these three textures are developed in the experimental material (Figs. 4 and 5).

In this study laboratory dedolomitization produced replacement of dolomite crystals by multiple calcite crystals in optical continuity, having an anhedral, interlocking crystal texture. At lower temperatures, the petrographic texture was dominated by irregular inclusions of dolomite in the centers of euhedral calcite crystals. In addition, the calcite-dolomite interfaces were generally angular but parallel with the original dolomite crystal face. The texture reflects the growth of calcite crystals into void space away from nucleation sites on the dissolving dolomite.

At higher temperatures, pseudomorphic replacement of dolomite by calcite is believed to be the dominant process, producing the most diagnostic dedolomitization textures. Islands of unreplaced dolomite commonly remain as inclusions in the calcite. The calcite-dolomite interfaces were more rounded than those produced at lower temperatures and were generally not parallel to the original dolomite crystal faces. Calcite replacement also occurs within the interior of the dolomite crystals, in association with crystal imperfections. Interior replacement of dolomite by calcite is commonly observed in ancient dolomites and has generally been attributed to an unstable calcium-rich core surrounded by a more stable dolomite rim. Our results imply temperature and crystal imperfections should also be considered in interpretating the causes of "zonal" dedolomitization.

SUMMARY

Seven week dedolomitization experiments at 100°, 150°, and 200°C in chloride brines containing 2 m Na and 0.5 m Ca, resulted in final aqueous molar ratios of Ca:Mg of 14.2, 23.5, and 35.4, respectively. Solution data imply equilibrium was reached at 150° and 200°C, and approached at 100°C. The 150° and 200°C results support those predicted based on the 25°C standard state data of HELGESON *et al.* (1978, 1981) for equilibrium between calcite and ordered dolomite. Sr distribution coefficients in the precipitated calcite showed a marked increase with temperature, being 0.027, 0.048, and 0.063, respectively, at 100°, 150°, and 200°C. This temperature dependence has not been verified in other studies at lower temperatures.

Between 100° and 200°C, the mode of calcite replacement of the dissolving dolomite changed from crystal growth into void space created by dolomite dissolution to pseudomorphic replacement of the dolomite. The dedolomitization textures of the laboratory samples demonstrated the validity of previously used thin section textural criteria for the identification of past dedolomitization events. However, less of these key textural features are preserved in the dissolution and precipitation mode of lower temperature dedolomitization events, suggesting the importance of low temperature dedolomitization may be underestimated.

Acknowledgements—Funding for this study was provided by AMOCO Production Company, EXXON Production Research Company, the Applied Carbonate Research Program at Louisiana State University, and Mobil Research and Development Corporation. The study was developed through discussions with Clyde Moore, Jeffrey Dravis, Richard Koepnick and David Eby. Technical help was supplied by Walter Holzwarth and Tim Klett of EXXON Production and Research Company. We appreciate the constructive reviews provided by the following journal reviewers: S. E. Drummond, M. W. Bodine, Jr. and L. N. Plummer.

Editorial handling: T. Pačes

REFERENCES

BACK W., HANSHAW, B. B., PLUMMER L. N., RAHN P. H., RIGHTMIRE C. T. and RUBIN M. (1983) Process and rate of dedolomitization: Mass transfer and ^{14}C dating in a regional carbonate aquifer. *Geol. Soc. Amer. Bull.* **94,** 1415–1429.

BAKER P. A. and KASTNER M. (1981) Constraints on the formation of sedimentary dolomite. *Science* **213,** 214–216.

BERNER R. A. (1981) Kinetics of weathering and diagenesis. In *Kinetics of Geochemical Processes* (eds. A. C. LASAGA and R. J. KIRKPATRICK), *Reviews in Mineralogy,* Vol. 8, pp. 111–133.

BRAUM M. and FRIEDMAN G. M. (1969) Dedolomites in peels: A possible clue to unconformity surfaces. *J. Sediment. Petrol.* **40,** 417–419.

BUDAI J. M., LOHMANN K. C. and OWEN R. M. (1984) Burial dedolomite in the Mississippian Madison Limestone, Wyoming and Utah thrust belt. *J. Sediment. Petrol.* **54,** 276–288.

CARPENTER A. B., TROUT M. L. and PICKETT E. E. (1974) Preliminary report on the origin and chemical evolution of lead- and zinc-rich oil field brines in central Mississippi. *Econ. Geol.* **69,** 1191–1206.

CHILINGAR G. V. (1956) Dedolomitization: A review. *Amer. Assoc. Petrol. Geol. Bull.* **40,** 762–778.

GOLDSMITH J. R. and GRAF D. L. (1958) Structural and compositional variations in some natural dolomites. *J. Geol.* **66,** 678–693.

HARVIE C. E. and WEARE J. H. (1980) The prediction of mineral solubilities in natural waters: the Na-K-Mg-Ca-Cl-SO_4-H_2O system from zero to high concentration at 25°C. *Geochim. Cosmochim. Acta* **44,** 981–997.

HARVIE C. E., MØLLER N. and WEARE J. H. (1984) The prediction of mineral solubilities in natural waters: the Na-K-Mg-Ca-H-Cl-SO_4-OH-HCO_3-CO_3-CO_2-H_2O system to high ionic strengths at 25°C. *Geochim. Cosmochim. Acta* **48,** 723–751.

HELGESON H. C., DELANY J. M., NESBITT H. W. and BIRD D. K. (1978) summary and critique of the thermodynamic properties of rock-forming minerals. *Amer. J. Sci.* **278-A,** 229 p.

HELGESON H. C., KIRKHAM D. H. and FLOWERS G. C. (1981) Theoretical prediction of the thermodynamic behavior of aqueous electrolytes at high pressures and temperatures: IV. Calculation of activity coefficients, osmotic coefficients, and apparent molal and standard and relative partial molal properties to 600°C and 5 kb. *Amer. J. Sci.* **281,** 1249–1516.

HOLLAND H. D., HOLLAND H. J. and MUNOZ J. L. (1964) The coprecipitation of cations with $CaCO_3$—II. The coprecipitation of Sr^{+2} with calcite between 90° and 100°C. *Geochim. Cosmochim. Acta* **28,** 1287–1301.

HOLMES H. F. and MESMER R. E. (1981) Isopiestic studies of aqueous solutions at elevated temperatures V. $SrCl_2$ and $BaCl_2$. *J. Chem. Thermo.* **13,** 1025–1033.

HOLMES H. F., BAES C. F. JR. and MESMER R. E. (1978) Isopiestic studies of aqueous solutions at elevated temperatures I. KCl, $CaCl_2$ and $MgCl_2$. *J. Chem. Thermo.* **10,** 983–996.

HOLMES H. F., BAES C. F., JR. and MESMER R. E. (1981) Isopiestic studies of aqueous solutions at elevated temperatures III. ((1-*y*)NaCl + *y*$CaCL_2$). *J. Chem. Thermo.* **13,** 101–113.

JACOBSON R. L. and USDOWSKI H. E. (1976) Partitioning of strontium between calcite, dolomite and liquids: An experimental study under higher temperature diagenetic conditions, and a model for the prediction of mineral pairs for geothermometry. *Contrib. Mineral. Petrol.* **59,** 171–185.

KASTNER M. (1982) When does dolomitization occur and what controls it (abstr). *11th Int'l Congress Sedimentology,* Hamilton, Ontario, Canada, 124.

KATZ A. (1968) Calcian dolomites and dedolomitization. *Nature* **217,** 439–440.

KATZ A., SASS E. and STARINSKY A. (1972) Strontium behavior in the aragonite-calcite transformation: An experimental study at 40–98°C. *Geochim. Cosmochim. Acta* **36,** 481–496.

KHARAKA Y. K., CALLENDER E. and WALLACE R. H., JR. (1977) Geochemistry of geopressured geothermal waters from the Frio Clay in the Gulf Coast region of Texas. *Geology* **5,** 241–244.

LAFON G. M. (1978) Discussion of "Equilibrium criteria for two-component solids reacting with solid composition in an aqueous phase—example: the magnesium calcites" by D. C. Thorstenson and L. N. Plummer. *Amer. J. Sci.* **274,** 61–83.

LAND L. S. and PREZBINDOWSKI D. R. (1981) The origin and evolution of saline formation water, Lower Cretaceous carbonates, south-central Texas, U.S.A. *J. Hydrology* **54,** 51–74.

LAND L.S. and PREZBINDOWSKI D. R. (1985) Chemical constraints and origins of four groups of Gulf Coast reservoir fluids: Discussion. *Amer. Assoc. Petrol. Geol. Bull.* **69,** 119–121.

LANGMUIR D. L. (1971) The geochemistry of some carbonate groundwaters in central Pennsylvania. *Geochim. Cosmochim. Acta* **35,** 1023–1045.

LORENS R. B. (1981) Sr, Cd, Mn and Co distribution coefficients in calcite as a function of calcite precipitation rate. *Geochim. Cosmochim. Acta* **45,** 553–561.

MILLER K. W. and HILDEBRAND J. H. (1968) Solutions of inert gases in water. *J. Amer. Chem. Soc.* **90,** 3001–3004.

PITZER K. S. (1979) Theory: ion interaction approach. In *Activity Coefficients in Electrolyte Solutions* (ed. R. M. PYTKOWICZ) Vol. I, pp. 157–208. CRC Press.

RAO C. G. (1969) Dolomitization, dedolomitization and the dolomite question in carbonate rocks. In *Selected Lectures on Petroleum Exploration,* Vol. 1, pp. 209–216, Petroleum Geology, Geophysics and Geochemistry, Institute Petrol. Explor., Oil Natural Gas Comm., Dehra Dun, India.

REEDER R. J. (1981) Electron optical investigation of sedimentary dolomites. *Contrib. Mineral. Petrol.* **76,** 148–157.

ROBIE R. A., HEMINGWAY B. S. and FISHER J. R. (1979) Thermodynamic properties of minerals and related substances at 298.15 K and 1 bar (10^5 Pascals) pressure and at higher temperatures. *U.S. Geol. Surv. Bull. No. 1452,* 456 p.

ROSENBERG P. E. and HOLLAND H. D. (1964) Calcite-dolomite-magnesite stability relations in solutions at elevated temperatures. *Science* **145,** 700–701.

ROSENBERG P. E., BURT D. M. and HOLLAND H. D. (1967) Calcite-dolomite-magnesite stability relations in solutions—the effect of ionic strength. *Geochim. Cosmochim. Acta* **31,** 391–396.

STOESSELL R. K. and BYRNE P. (1982) Salting-out of methane in single-salt solutions at 25°C and below 800 psia. *Geochim. Cosmochim. Acta* **46,** 1327–1332.

STOESSELL R. K. and MOORE C. H. (1985) Chemical constraints and origins of four groups of Gulf Coast Reservoir Fluids: Reply. *Amer. Assoc. Petrol. Geol. Bull.* **69,** 122–126.

WEISS R. F. (1970) The solubility of nitrogen, oxygen and argon in water and seawater. *Deep-Sea Res.* **17,** 721–735.

WOOD S. A., CRERAR D. A., BRANTLEY S. L. and BORCSIK M. (1984) Mean molal stoichiometric activity coefficients of alkali halides and related electrolytes in hydrothermal solutions. *Amer. J. Sci.* **284,** 668–705.